TLR2 Plays a Pivotal Role in Mediating Mucosal Serotonin Production in the Gut

Huaqing Wang, Yun Han Kwon, Varun Dewan, Fatemeh Vahedi, Saad Syed, Michelle E. Fontes, Ali A. Ashkar, Michael G. Surette and Waliul I. Khan

This information is current as of January 24, 2022.

Supplementary Material	http://www.jimmunol.org/content/suppl/2019/04/04/jimmunol.1801034.DCSupplemental
References	This article **cites 61 articles**, 13 of which you can access for free at: http://www.jimmunol.org/content/202/10/3041.full#ref-list-1

Why *The JI*? Submit online.

- **Rapid Reviews! 30 days*** from submission to initial decision

- **No Triage!** Every submission reviewed by practicing scientists

- **Fast Publication!** 4 weeks from acceptance to publication

*average

Subscription	Information about subscribing to *The Journal of Immunology* is online at: http://jimmunol.org/subscription
Permissions	Submit copyright permission requests at: http://www.aai.org/About/Publications/JI/copyright.html
Email Alerts	Receive free email-alerts when new articles cite this article. Sign up at: http://jimmunol.org/alerts

TLR2 Plays a Pivotal Role in Mediating Mucosal Serotonin Production in the Gut

Huaqing Wang,*,†,1 Yun Han Kwon,*,†,1 Varun Dewan,*,†,1 Fatemeh Vahedi,*,‡
Saad Syed,§,¶ Michelle E. Fontes,†,§,¶ Ali A. Ashkar,*,‡ Michael G. Surette,†,‡,§,¶ and
Waliul I. Khan*,†

Serotonin (5-hydroxytryptamine [5-HT]) is a key enteric signaling molecule that mediates various physiological processes in the gut. Enterochromaffin (EC) cells in the mucosal layer of the gut are the main source of 5-HT in the body and are situated in close proximity to the gut microbiota. In this study, we identify a pivotal role of TLR2 in 5-HT production in the gut. Antibiotic treatment reduces EC cell numbers and 5-HT levels in naive C57BL/6 mice, which is associated with downregulation of TLR2 expression but not TLR1 or TLR4. TLR2-deficient ($Tlr2^{-/-}$) and $Myd88^{-/-}$ mice express lower EC cell numbers and 5-HT levels, whereas treatment with TLR2/1 agonist upregulates 5-HT production in irradiated C57BL/6 mice, which are reconstituted with $Tlr2^{-/-}$ bone marrow cells, and in germ-free mice. Human EC cell line (BON-1 cells) release higher 5-HT upon TLR2/1 agonist via NF-κB pathway. $Tlr2^{-/-}$ mice and anti-TLR2 Ab–treated mice infected with enteric parasite, *Trichuris muris*, exhibited attenuated 5-HT production, compared with infected wild-type mice. Moreover, excretory-secretory products from *T. muris* induce higher 5-HT production in BON-1 cells via TLR2 in a dose-dependent manner, whereby the effect of excretory-secretory products is abrogated by TLR2 antagonist. These findings not only suggest an important role of TLR2 in mucosal 5-HT production in the gut by resident microbiota as well as by a nematode parasite but also provide, to our knowledge, novel information on the potential benefits of targeting TLR2 in various gut disorders that exhibit aberrant 5-HT signaling. *The Journal of Immunology*, 2019, 202: 3041–3052.

The human gastrointestinal (GI) tract contains the largest endocrine system in the body, which is essential for control of motility and secretion as well as the expulsion of harmful pathogens and toxins (1). There are at least 14 types of enteroendocrine cells (EECs) in the GI tract that are responsible for secretion of more than 100 biologically active peptides (1, 2). The most populous of the EECs are the enterochromaffin (EC) cells, whose primary secretory product is serotonin, also known as 5-hydroxytryptamine (5-HT) (3). About 95% of the body's 5-HT is found within the gut with EC cells being its main reservoir, although some are produced by enteric neurons and mast cells (3). Tryptophan hydroxylase 1 (Tph1), the rate-limiting enzyme for 5-HT biosynthesis in EC cells, catalyzes the conversion of dietary L-tryptophan into 5-hydroxytryptophan (5-HTP), which is further converted to 5-HT by aromatic L-amino acid decarboxylase and subsequently stored in granules prior to secretion via exocytosis in a calcium-dependent manner (3). 5-HT is secreted into lamina propria and the lumen in response to mechanical and various chemical stimuli including bacterial toxins (4–6). Secreted 5-HT acts on many targets including enteric neurons, smooth muscle cells, immune cells and enterocytes via several 5-HT receptors, regulating various functions in the GI tract (7).

5-HT is considered as an important signaling molecule in maintaining GI homeostasis. Changes in EC cell numbers and 5-HT have been observed in a number of GI diseases including inflammatory bowel disease (IBD) and irritable bowel syndrome (IBS) as well as in animal models of various enteric infections, including with the helminth parasite, *Trichuris muris* (8–14). Recently, we reported the reduced severity of colitis and downregulated production of proinflammatory cytokines in *Tph1*-deficient ($Tph1^{-/-}$) mice, which have significantly reduced 5-HT in the gut compared with wild-type (WT) mice after dextran sulfate sodium (DSS)– and 2,4-dinitrobenzenesulfonic acid–induced colitis (15). Extending these findings, we discovered that blocking peripheral Tph1 with a pharmacological agent (LX1032/LX1606) attenuated the severity of both DSS- and *T. muris* infection–induced colitis, further revealing roles for 5-HT in exacerbating the severity of colitis (16).

*Department of Pathology and Molecular Medicine, McMaster University, Hamilton, Ontario L8S 4K1, Canada; †Farncombe Family Digestive Health Research Institute, McMaster University, Hamilton, Ontario L8S 4K1, Canada; ‡McMaster Immunology Research Centre, Michael G. DeGroote Institute for Infectious Disease Research, McMaster University, Hamilton, Ontario L8S 4K1, Canada; §Department of Biochemistry and Biomedical Sciences, McMaster University, Hamilton, Ontario L8S 4K1, Canada; and ¶Department of Medicine, McMaster University, Hamilton, Ontario L8S 4K1, Canada

[1]H.W., Y.H.K., and V.D. contributed equally to this work.

ORCIDs: 0000-0002-4232-9141 (Y.H.K.); 0000-0001-7377-2835 (F.V.); 0000-0003-1139-1468 (A.A.A.).

Address correspondence and reprint requests to Dr. Waliul I. Khan, McMaster University Medical Center Room 3N7, 1280 Main Street West, Hamilton, ON L8S 4K1, Canada. E-mail address: khanwal@mcmaster.ca

The online version of this article contains supplemental material.

Abbreviations used in this article: BMC, bone marrow cell; DSS, dextran sulfate sodium; EC, enterochromaffin; EEC, enteroendocrine cell; ESP, excretory-secretory product; FSC, forward scatter; GF, germ-free; GI, gastrointestinal; 5-HT, 5-hydroxytryptamine; IBD, inflammatory bowel disease; IBS, irritable bowel syndrome; MyD88, myeloid differentiation primary response 88; SPF, specific pathogen–free; SSC, side scatter; Tph1, tryptophan hydroxylase 1; v3, variable 3; WT, wild-type.

Many components of the luminal microenvironment have the potential to stimulate the release of 5-HT from EC cells. The GI tract is colonized by a complex, heterogeneous, and dynamic microbial ecosystem, containing up to 1×10^{14} CFU of bacteria (17). Previous studies provide evidence that *Trichuris* species adapt to exist in the colon and interact with the commensal microbiota, which subsequently affect host immune regulation (18–21). Because of the close proximity of EC cells to the gut microbiome, it is very likely that the interaction between microorganisms and EC cells plays an important role in GI pathology and pathophysiology. It is demonstrated that indigenous spore-forming gut bacteria induces 5-HT production and *Tph1* expression in colonic EC cells (22). Moreover, short-chain fatty acids, which are metabolic by-products of bacterial fermentation, have been shown to stimulate the release of 5-HT in rat colon ex vivo (23). Regardless of significant advances, it is not yet fully understood as to how microbes influence EC cell biology to regulate 5-HT production.

TLRs are important components of the host innate immune system and play a critical role for intestinal homeostasis through the detection of various pathogen-associated molecular patterns (24). A recent study has revealed diversity in the temporal and spatial patterns of TLR expression, whereby expression of TLR1, TLR2, and TLR4 are much greater in the colon as compared with other TLRs (25). In addition, the expression of TLR1, TLR2, and TLR4 was shown in human and murine EC cells (26). However, despite a significant increase in the knowledge of TLRs in microbial infections over the years, their role in mediating microbiota/pathogen-associated molecular pattern–induced 5-HT production is still modest.

In this study, we describe the important role of TLR signaling in regulating gut 5-HT production. Studies with BON-1 cells reveal an increase in *Tph1* expression and 5-HT release in an NF-κB–dependent manner upon stimulation with TLR2/1 agonist. In vivo studies involving $Tlr2^{-/-}$, $Tlr4^{-/-}$, myeloid differentiation primary response 88 ($MyD88^{-/-}$), $Tph1^{-/-}$, and germ-free (GF) mice demonstrate a pivotal role of TLR2 in regulating *Tph1*-mediated 5-HT production. In addition, a bone marrow chimera experiment revealed that TLR2 in nonhematopoietic cells, potentially in intestinal epithelial cells, is necessary to stimulate 5-HT production in the gut. Finally, using the enteric parasite *T. muris* model, we unveil an important role of TLR2 in mediating changes in colonic 5-HT levels. Taken together, our study identifies a novel role of TLR2 in regulating 5-HT production in the gut.

Materials and Methods
Mice

Congenic C57BL/6 (CD45.1), $Tlr2^{-/-}$, $Tlr4^{-/-}$, and $MyD88^{-/-}$ and age-matched (8–10 wk of age) WT (C57BL/6 background) counterparts were purchased from The Jackson Laboratory. Breeding pairs of $Tph1^{-/-}$ and $Tph1^{+/+}$ mice were obtained from CNRS, Paris, France, and were kept and bred under specific pathogen–free (SPF) conditions of central animal facility. All mice were housed in sterilized, filter-topped cages, fed autoclaved normal chow food at a temperature of 21–22°C, and with 12:12 h light/dark cycle in an SPF room of McMaster University central animal facility. All mice were acclimatized for 10 d prior to the start of any experiments. GF mice (C57BL/6 background) were obtained from the Farncombe Gnotobiotic Unit of McMaster University. Male mice were used for all experiments, and the experiments were approved by the Animal Research Ethics Board of McMaster University and conducted under the Canadian guidelines for animal research.

Antibiotics

C57BL/6 mice received either antibiotics (10 mg/ml neomycin or 0.5 mg/ml vancomycin dissolved in sterilized water) or sterilized water. The experiment lasted 7 d, during which time weight, water, and food intake were recorded, and daily s.c. saline injections were administered to all mice to prevent dehydration. At day 7, mice were sacrificed, and colonic, cecal, and fecal samples were collected for further analysis.

Bioinformatics and 16s rRNA sequencing

Fecal and cecal samples from antibiotic-treated and control mice were stored at −80°C. DNA was extracted and the 16S rRNA variable 3 (v3) gene region was amplified as previously described (27). Briefly, samples were thawed to room temperature. Approximately 300 μl of sample was suspended in 800 μl of 200 mM NaPO₄ (pH 8), and 100 μl of guanidine thiocyanate-EDTA–Sarkosyl along with 0.2 g of 0.1 mm glass beads (Mo Bio Laboratories, Carlsbad, CA). Sample mixtures were homogenized at 3000 RPM for 3 min. Enzymatic lysis was performed using 50 μl lysozyme (100 mg/ml), 50 μl mutanolysin (10 U/ml), 10 μl RNase A (10 mg/ml), and incubation at 37°C for 90 min. Next, 25 μl of 25% NaDodSO₄ (SDS), 25 μl of proteinase K, and 62.5 μl of 5 M NaCl were added to the sample and incubated at 65°C for 90 min. Following, samples were pelleted at $13,500 \times g$ for 5 min by centrifugation and the supernatant was transferred to a new microcentrifuge tube containing 900 μl of phenol/chloroform/isoamyl alcohol. The tube was then mixed at 13,500 g for 10 min. The least dense layer was transferred to a new microcentrifuge tube, and DNA from this layer was extracted using the Zymo DNA Clean and Concentrator 25 Kit (Zymo Research, Irvine, CA). DNA was eluted using 50 μl of sterilized water. The 16S rRNA v3 gene region was amplified using 341F and 518R 16S rRNA primers modified for the Illumina platform with adaptors containing 6-bp unique barcodes to the reverse primer. PCR amplification was adapted from a previous study (28). Each sample reaction mixture contained 5 pmol of each primer, 200 μM of each deoxynucleoside triphosphate (dNTP), 1.5 mM MgCl₂, and 1 U *Taq* polymerase (Life Technologies, Carlsbad, CA). The PCR protocol consisted of an initial denaturation step at 95°C for 5 min, 30 cycles, each step for 30 s, of 95, 50, and 72°C, and a final extension step at 72°C for 7 min. Amplification of the v3 gene region was verified by electrophoresis on a 2% agarose gel. Amplicons were then sequenced using the Illumina MiSeq platform. Resulting paired-end sequences from Illumina sequencing were processed using a custom in-house pipeline (29). Briefly, this pipeline uses Cutadapt to trim any reads surpassing the length of the v3 region, PANDAseq to align the paired-end sequences, Sickle to quality-filter sequences, QIIME to size filter for sequences between 100 and 250 bp and to check for and remove chimeras, AbundantOTU+ (clustering threshold of 97%; 17) to pick operational taxonomic units, and Ribosomal Database Project classifier to assign taxonomy using the Greengenes reference database (30). To measure β-diversity, samples were normalized. Analysis was conducted using the phyloseq and vegan packages on R and using GraphPad Prism version 6.0 for Mac OS X (GraphPad Software, La Jolla, CA).

BON-1 cell culture

BON-1 cells (human carcinoid cell line derived from a metastasis of a pancreatic carcinoid tumor of EC cell origin) were cultured in DMEM supplemented with 10% FBS and 1% penicillin/streptomycin. Briefly, cells were seeded at 5×10^5 cells per well in a 12-well plate and incubated for 24 h at 37°C in the complete growth medium. The medium was replaced with serum-free media prior to treatment. Unless otherwise mentioned, all concentrations used for the treatments are: 2, 5, and 10 μg/ml Pam3CSK4 (TLR2/1 agonist; InvivoGen, San Diego, CA), 10, 50, and 100 ng/ml LPS (TLR4 agonist; InvivoGen), 1 μM CU-CPT22 (TLR2 antagonist; Millipore Sigma, Oakville, Canada) 1 mM sodium butyrate (Sigma-Aldrich, Oakville, Canada), 20 nM triptolide (NF-κB inhibitor; Tocris Biosciences, Burlington, Canada), and 1 μM SR 11302 (AP-1 inhibitor; Tocris Biosciences). Following the treatment, the cell supernatants and RNA were collected and stored at −80°C for further analysis.

5-HT ELISA

5-HT levels were determined as previously described (16, 31). Briefly, colonic tissues and feces were weighed and homogenized in 0.2 N perchloric acid. Following centrifugation at $10,000 \times g$ for 5 min, the supernatants were collected, and the pH was neutralized using 1 M borate buffer. The supernatants were used for analysis of 5-HT levels using commercially available ELISA kits (Beckman Coulter, Fullerton, CA). 5-HT content was expressed as a function of weight (nanograms per milligram). For in vitro experiments, the obtained cell supernatants were diluted with the dilution buffer provided in the manufacturer's kit, and 5-HT concentrations were expressed as nanomolars.

Immunohistochemistry

Immunohistochemical studies of 5-HT–expressing EC cells were performed on paraffin wax–embedded colonic sections, as previously described (15, 16).

Primary Ab used for 5-HT was a rabbit anti–5-HT Ab (Immunostar, Hudson, WI). Immunostained sections were observed at 200× magnification, and the numbers of 5-HT–positive EC cell were expressed as the number of positive cells per 10 crypts. To count EC cells, slides were visualized at 40× magnification and at least 40 random crypts at the top, bottom, and both sides of each image were used to count the number of cells that were 5-HT positive. If the section is in poor condition (<25% damaged), one of the four sections is counted on the opposite side. If >25% of section is damaged, the section is not counted.

Anti-TLR2 treatment

C57BL/6 mice were i.p. treated with either anti-IgG (purified mouse IgG1, κ isotype control Ab; BioLegend, San Diego, CA) or anti-TLR2 Ab (purified anti-mouse/human CD282 Ab; BioLegend) at a dosage of 200 μg/kg (32) starting from 1 d before infection.

Bone marrow chimeras

Bone marrow cells (BMCs) was collected from the femurs and the tibiae of C57BL/6 (CD45.1) and $Tlr2^{-/-}$ (CD45.2). BMCs were depleted of T cells using anti-CD4 (clone GK1.5) (Bio X Cell, Cedarlane, Burlington, Canada), anti-CD8 (clone 2.43) (Bio X Cell), and anti-Thy1.2 (clone 30H12) (Bio X Cell) at 4°C for 1 h, followed by treatment with Low-Tox-M guinea pig complement at 37°C for 1 h. Recipient mice were irradiated with two doses of 550 rad with a 3 h interval between irradiations via a ^{137}Cs γs7se radiation source (γ Cell 40; Nordion, Kanata, Canada) and reconstituted via tail vein with 10^7 T cell–depleted BMCs after the second dose of radiation. Recipient mice received antibiotics (Septra) in drinking water for 2 wk after irradiation and were monitored until week 6.

Flow cytometry

Blood samples were taken from the facial vein into a 1.5-ml tube containing anticoagulant. RBCs were removed using Ammonium-Chloride-Potassium Lysing Buffer (Life Technologies, Grand Island, NY). Cell suspensions were resuspended in a 0.2% BSA PBS solution, and nonspecific Ab binding was blocked with anti-CD16/CD32 Ab (eBioscience, San Diego, CA). Extracellular cell staining was conducted by using combinations of allophycocyanin–conjugated anti-CD45.1 and FITC–conjugated anti-CD45.2. Stained cells were analyzed on an LSRFortessa Flow Cytometry System (BD Biosciences). In this sample gating, cells were first gated for singlets (forward scatter [FSC]-H versus FSC-A and side scatter [SSC]-H versus SSC-A) and lymphocytes (SSC-A versus FSC-A). The lymphocyte gate is further analyzed for their expression of CD45.1 and CD45.2. Data were acquired using a FACSCanto flow cytometer with FACSDiva 5.0.2 software (BD Pharmingen) and analyzed with FlowJo Mac.

Quantitative real-time-PCR

Colonic tissues were homogenized with TRIzol reagent (Invitrogen, Burlington, Canada) using a Mixer Mill (MM 400, Retsch, Newtown, PA) at 30 frequency for 5 min. Total RNA from BON-1 cells was extracted using an RNeasy Midi kit (QIAGEN, Toronto, Canada). Total RNA was quantified using a NanoDrop 2000 spectrophotometer (Thermo Fischer Scientific, Mississauga, Canada). RNA purity was assessed by the ratio of absorbance at 260/280 nm, and only samples with a ratio of ~2.0 for RNA were considered. cDNA was prepared from 1 μg of total RNA using iScript cDNA Synthesis Kit (Bio-Rad Laboratories, Mississauga, Canada). Relative quantitative RT-PCR amplification was performed using SsoFast EvaGreen Supermix (Bio-Rad Laboratories) with the following primers at a concentration of 10 μM, and the cycling conditions used were previously described: mouse *Tph1* (forward: 5′-CAC GAG TGC AAG CCA AGG TTT-3′; reverse: 5′-AGT TTC CAG CCC CGA CAT CAG-3′) (33); mouse *Tlr2* (forward: 5′-CCA AAG AGC TCG TAG CAT CC-3′; reverse: 5′-AGG GGC TTC ACT TCT CTG CT-3′) (34); mouse *Tlr4* (forward: 5′-GGA AGA ACA AGA AAC GGC AAC T-3′; reverse: 5′-CAT AGC AGA GCC CCA GGT GA-3′) (35) and mouse *Tlr1* (forward: 5′-CAA TGT GGA AAC AAC GTG GA-3′; reverse: 5′-TGT AAC TTT GGG GGA AGC TG-3′) (36); mouse *Math1* (forward: 5′-GTG CGA TCT CCG AGT GAG AG-3′; reverse: 5′-GGG ATA AGC CCC GAA CAA CA-3′) (37); human *Tph1* (forward: 5′-TGC CCT TGC TAA GGT CAG CAG GA-3′; reverse: 5′-AGC AAG AGA TGG CCC AGA CCT CC-3′) (38); human *Tlr2* (forward: 5′-CAG GTG ACT GCT CGG AGT TC-3′; reverse: 5′-CAC AAC TAC CAG TTG AAA GCA GTG A-3′) (39). Multiple classical internal control genes for mouse and human, such as 18S rRNA and GAPDH, respectively, were used as an internal standard as previously described (40, 41). Data were analyzed according to the $2^{-\Delta\Delta CT}$ method and expressed as relative abundances (mean ± SEM).

Western blot

BON-1 cells were isolated in RIPA buffer containing protease inhibitor (Sigma-Aldrich). Equal amounts of protein homogenates from each group were loaded and electrophoresed onto a 4–15% Mini-PROTEAN TGX Precast Protein Gel (Bio-Rad Laboratories) and transferred to a PVDF membrane using Transblot turbo transfer system (Bio-Rad Laboratories) as per the manufacturer's instructions. The membrane was blocked with 3% BSA blocking buffer for 1.5 h at room temperature and incubated with primary Ab against TLR2 (1:1000) (06-1119; EMD Millipore, Etobicoke, Canada) overnight at 4°C. The membrane was washed and incubated with anti-rabbit HRP-linked Ab (1:5000; Cell Signaling Technology) for 1 h at room temperature. Proteins were visualized by use of SuperSignal West Femto Maximum Sensitivity Substrate (Thermo Fisher Scientific, Burlington, Canada). The membrane of the experimental blot was stripped by Restore PLUS Western blot Stripping Buffer (Thermo Fisher Scientific). β-actin was used as a loading control from a stripped and reprobed membrane of the experimental blot shown. Densitometric analysis was performed on Western blots with ImageJ software (version 1.48), normalized to total actin. Total protein concentration of homogenized tissue was determined using DC Protein Assay Kit (Bio-Rad Laboratories) (42).

T. muris

Adult *T. muris* parasites were harvested, and ova was collected and maintained as previously described (41, 43). All infected mice received ~300 *T. muris* embryonated eggs by oral gavage. Infected mice were euthanized on day 16 postinfection and colon was removed to examine 5-HT levels, EC cells, cytokines, and worm burden, which was assessed by counting the number of worms present in the cecum as previously described (11, 12). BON-1 cells were treated with the excretory-secretory products (ESPs) from *T. muris*.

Statistical analysis

All statistical analysis, except for bioinformatics and 16s rRNA sequencing analysis, was performed using GraphPad Prism 5 (GraphPad Software, La Jolla, CA), and results are represented as either mean or mean ± SEM. Student *t* test and one-way ANOVA with Dunnett or Bonferroni multiple comparison test were used. A *p* value <0.05 was considered statistically significant.

Results

Antibiotic administration in mice attenuates intestinal TLR2 expression along with a reduction in 5-HT production

Aimed at understanding the effects of perturbing the gut microbiota on TLRs expression and 5-HT production, naive C57BL/6 mice were treated with either neomycin or vancomycin, and TLR expression and components of 5-HT signaling were investigated. Bacterial profiling of both fecal and cecal microbiota revealed significant differences in microbial composition postantibiotic (Fig. 1A, 1B). The fecal and cecal contents from each mouse were similar in composition. Neomycin reduced the relative abundance of *Allobactum*, *Lactobacillus*, *Anaeroplasma*, *Lachnospiriceae*, and *Ruminococcaceae* and expanded the relative abundance of *Parabacteroides* and *Akkermansia*. In most of the mice treated with neomycin, *Bacteroides* and *Alistipes* were also decreased, resulting in two distinct clusters of antibiotic-treated mice (Fig. 1B). Mice treated with vancomycin showed more variability between mice, but the larger shifts in microbiota composition (principal coordinate analysis in Fig. 1B) were similar to the neomycin-treated mice. Mice treated with vancomycin had reduced relative abundance of *Allobactum*, *Alistipes*, *Lachnospiriceaea*, and *Ruminococcaceae* and a similar expansion of *Parabacteroides* and *Akkermansia*. These findings demonstrate that treatment with antibiotics mostly diminished the relative abundance of Gram-positive bacteria (*Allobactum*, *Anaeroplsma*, *Lachnospiriceaea*, and *Ruminococcaceae*) and increased relative abundance of Gram-negative bacteria (*Parabacteroides* and *Akkermansia*).

In consort with altered microbial composition, we observed significantly reduced 5-HT–expressing EC cell numbers and colonic 5-HT levels in both antibiotic-treated mice, as compared
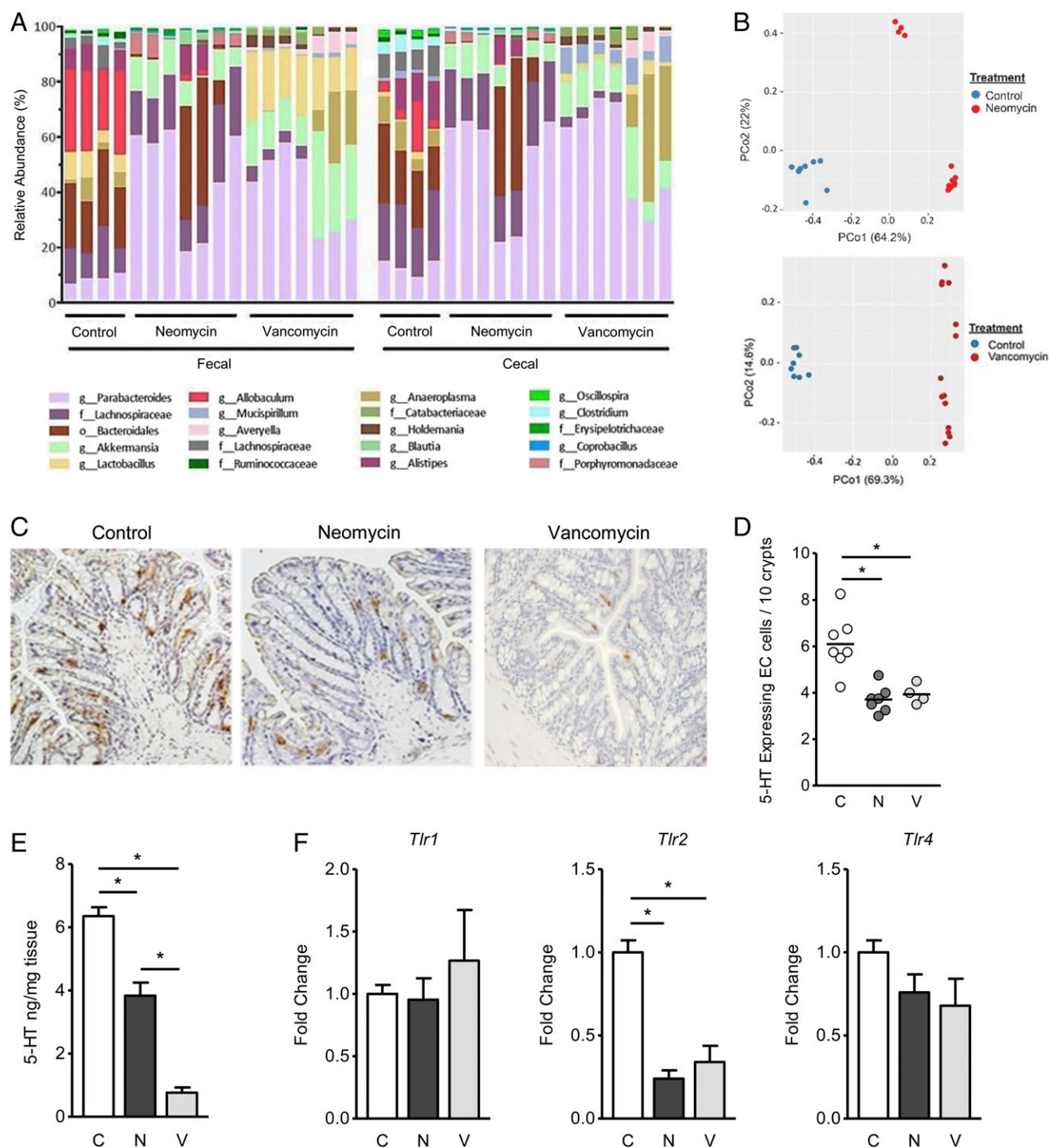
FIGURE 1. Effects of antibiotic administration on gut microbiota, 5-HT, and TLR2. C57BL/6 mice received either sterilized water (C = control) or antibiotics (10 mg/ml neomycin (N) or 0.5 mg/ml vancomycin [V]; $n = 4–7$ mice per group) in drinking water (sterilized water). The experiment lasted 7 d during which time weight, water, and food intake were recorded and daily s.c. saline injections were administered to all mice to prevent dehydration. At day 7, mice were sacrificed, and colonic, cecal, and fecal samples were collected for further analysis. (**A**) Relative abundance of genera that appeared >3% across all samples were visualized in the microbial analysis. (**B**) Principal coordinates analysis plots of the Bray–Curtis dissimilarity metric were colored by treatment, and PERMANOVA statistical testing revealed significant association by treatment in both cecal and fecal samples ($p = 0.00001$ for both plots). Numbers in brackets indicate the degree of variance explained by the PCo. PCo, principal coordinate. (**C**) Representative micrographs of 5-HT–expressing EC cells following immunostaining (brown) in the colonic sections of control, neomycin-, and vancomycin-treated mice. Colonic sections were visualized using a Nikon Eclipse 80i microscope (original magnification ×10). (**D**) 5-HT–expressing EC cells per 10 crypts in the colon. (**E**) 5-HT content in the colonic tissues as determined by ELISA. (**F**) Quantitative RT-PCR to determine colonic *Tlr1*, *Tlr2*, and *Tlr4* mRNA expression normalized to GAPDH reference gene. Unpaired Student *t* test and one-way ANOVA with Dunnett multiple comparisons were used to analyze statistical differences. Data are represented as either mean or mean ± SEM where applicable. *$p < 0.05$; n.s., not significant.

with controls (Fig. 1C–E). As EC cells have previously been shown to express functional TLR1, 2, and 4 (26), we investigated the expression of these innate receptors in colonic tissues of mice

with and without the antibiotic treatment. We observed no significant changes in TLR1 and TLR4 expression after treatment with antibiotics (Fig. 1F). However, a significant downregulation

of TLR2 expression in mice treated with both antibiotics was observed, compared with controls (Fig. 1F). These findings suggest an important role of TLR2 in mediating microbiota-induced 5-HT production.

Deficiency of TLR2 signaling impairs 5-HT production in vivo

To further demonstrate the involvement of TLR2 in regulating 5-HT production in vivo, we used a two-way approach. First, we used naive $Tlr2^{-/-}$ and $Tlr4^{-/-}$ mice to investigate 5-HT–expressing EC cells and 5-HT levels in the colon. We found $Tlr2^{-/-}$ mice express lower EC cell number and 5-HT levels in comparison with WT and $Tlr4^{-/-}$ mice (Fig. 2A–C). In addition, fecal 5-HT levels in $Tlr2^{-/-}$ mice were significantly lower compared with WT mice (Fig. 2D). Interestingly, we have not observed any differences in 5-HT levels and EC cell numbers in $Tlr4^{-/-}$ mice, as compared with that in WT mice. MyD88 is a central adaptor in majority of TLRs. We investigated whether other TLRs might contribute to 5-HT production by using $MyD88^{-/-}$ mice. Colonic 5-HT levels were significantly reduced in

$MyD88^{-/-}$ mice, compared with WT mice, whereas there was no significant difference in EC cell number, colonic 5-HT levels, or fecal 5-HT levels between $MyD88^{-/-}$ and $Tlr2^{-/-}$ mice (Fig. 2A–D). Math1 is a basic helix–loop–helix transcription factor important in differentiation of EECs from stem cells, and Tph1 is the rate-limiting enzyme in 5-HT synthesis in EC cells. We observed significantly lower expression of *Math1* (Fig. 2E) and *Tph1* (Fig. 2F) in $Tlr2^{-/-}$ and $Myd88^{-/-}$ mice, compared with WT mice, implying an important role that TLR2 deficiency is responsible for the differentiation of EC cells from stem cells and the regulation of the enzyme-mediated generation of 5-HT.

TLR2 signaling in the hematopoietic cell compartment is not required for 5-HT production

As TLR2 is also expressed in various leukocytes, we further investigated to demonstrate whether activation of TLR2 in the hematopoietic cells is required for 5-HT production. We generated chimeric mice by reconstituting WT and $Tlr2^{-/-}$ mice with BMCs
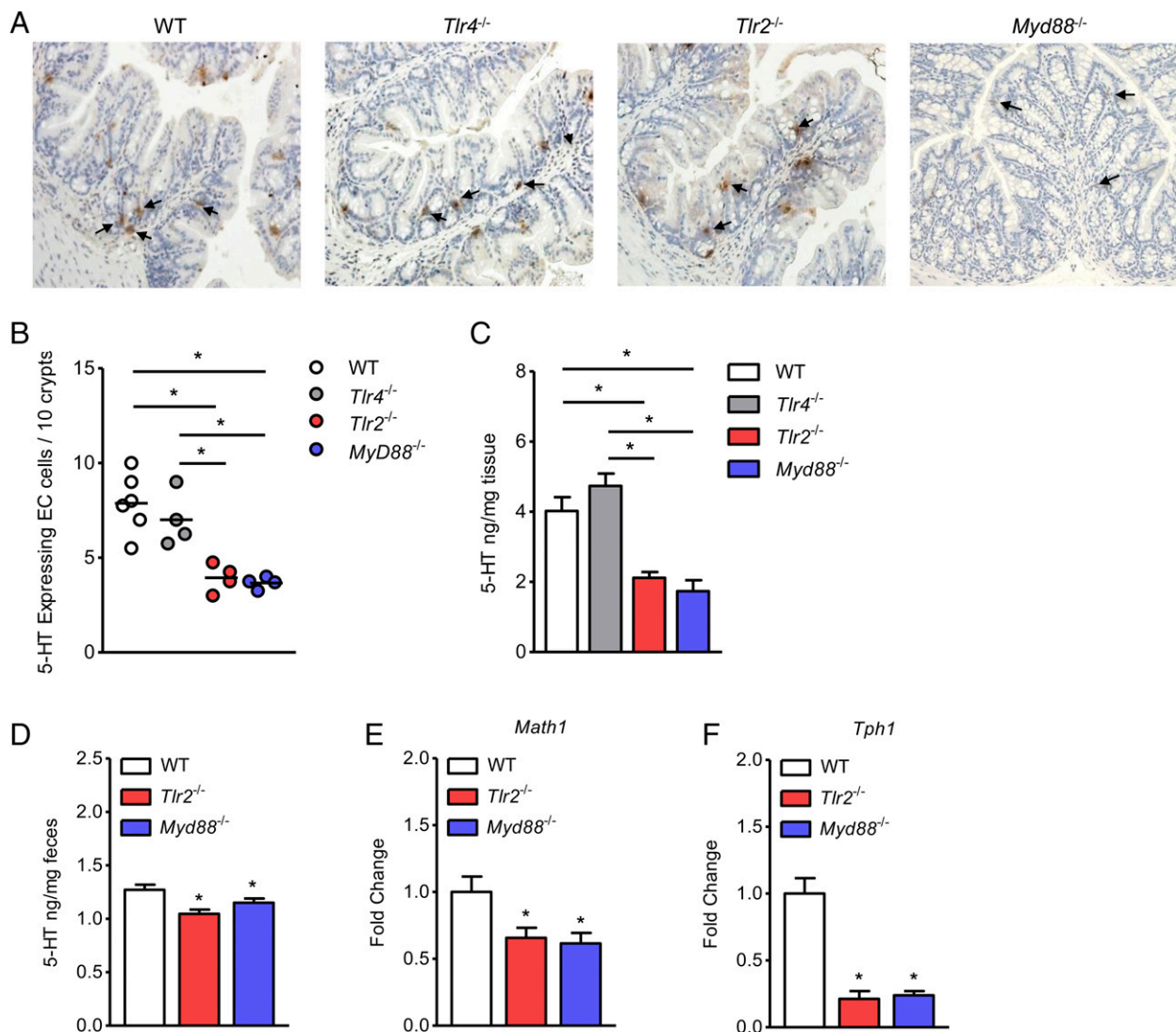

FIGURE 2. Abrogation of *Tlr2* reduces 5-HT production. (**A**) Representative micrographs of 5-HT–expressing EC cells following immunostaining (brown) in the colonic sections of C57BL/6 (WT), $Tlr2^{-/-}$, $Tlr4^{-/-}$, and $MyD88^{-/-}$ mice. Arrows indicate 5-HT–positive cells. Colonic sections were visualized using a Nikon Eclipse 80i microscope (original magnification ×10). (**B**) 5-HT–expressing EC cells per 10 crypts in the colon. (**C**) Colonic 5-HT content as determined by ELISA. (**D**) Fecal 5-HT concentration in WT, naive $Tlr2^{-/-}$, and $Myd88^{-/-}$ mice as determined by ELISA. Expression of *Math1* (**E**) and *Tph1* (**F**) mRNA in the colonic tissues of WT, naive $Tlr2^{-/-}$, and $Myd88^{-/-}$ mice ($n = 3–6$ mice per group). Unpaired Student t test and one-way ANOVA with Dunnett multiple comparisons were used to analyze statistical differences. Data are represented as either mean or mean ± SEM where applicable. *$p < 0.05$.

harvested from either WT or $Tlr2^{-/-}$ mice. Six weeks after reconstitution, all recipient mice were administered with Pam3CSK4 (3 doses of 100 μg i.p. every other day) (44) (Fig. 3A, 3B). $Tlr2^{-/-}$ mice reconstituted with WT BMCs still expressed lower EC cell number and secreted lower levels of 5-HT in the colon than WT mice reconstituted with

$Tlr2^{-/-}$ BMCs (Fig. 3C, 3D), suggesting that TLR2-mediated signaling in hematopoietic cells has no significant effect in promoting 5-HT secretion. These findings demonstrate that TLR2 signaling in the nonhematopoietic cells, most likely intestinal epithelial cells, is necessary to stimulate 5-HT production in the gut.
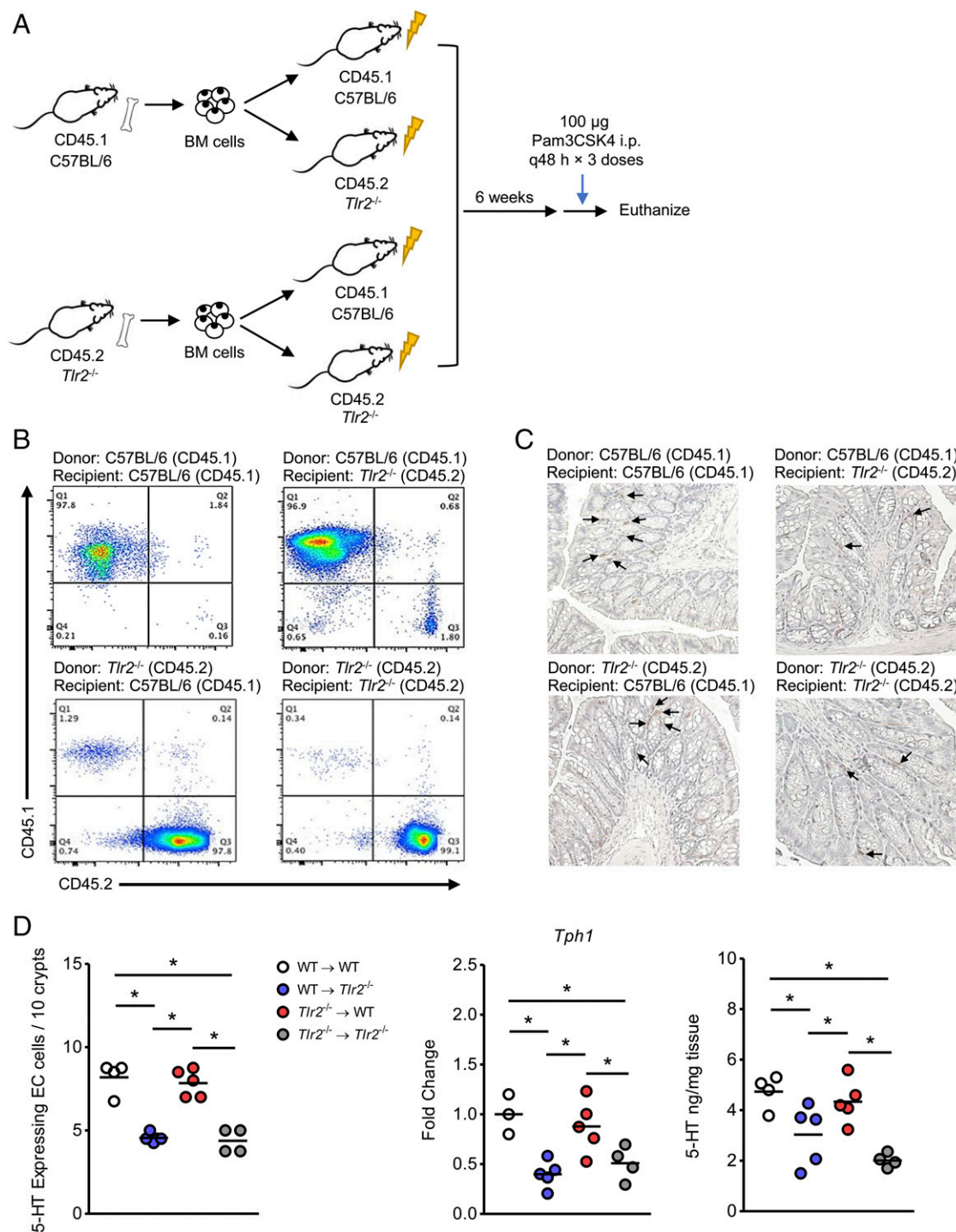
FIGURE 3. TLR2 signaling in the non-BMCs, potentially epithelial cells, but not in the hematopoietic cell compartment, is important in 5-HT production in gut. (**A**) Irradiated WT and $Tlr2^{-/-}$ mice were reconstituted with T cell–depleted BMCs harvested from the femurs and tibias of $Tlr2^{-/-}$ and WT mice, respectively. Six weeks after reconstitution, Pam3CSK4 was i.p. injected into the recipient mice every other day for three doses before euthanizing. (**B**) Flow cytometric analysis showing the assessment of peripheral blood for reconstitution through examination of the frequency of cells expressing CD45.1 or CD45.2. (**C**) Representative micrographs of 5-HT–expressing EC cells following immunostaining (brown) in the colonic sections of the recipient mice. Arrows indicate 5-HT–positive cells. Colonic sections were visualized using a Nikon Eclipse 80i microscope (original magnification ×10). (**D**) 5-HT–expressing EC cells per 10 crypts in the colon (left); *Tph1* expression in the colonic tissues (middle); colonic 5-HT content as determined by ELISA (right) ($n = 4–5$ mice per group). One-way ANOVA with Bonferroni multiple comparison was used to analyze statistical differences. Data are represented as either mean or mean ± SEM. $*p < 0.05$.

Administration of TLR2 agonist upregulates Tph1 *expression and 5-HT production in GF mice*

GF mice have been demonstrated to harbor lower levels of 5-HT in the colon in comparison with conventional mice (22, 31). We also observed significantly lower levels 5-HT and EC cell numbers in GF mice as compared with SPF mice (Supplemental Fig. 1). Based on our findings from antibiotic-treated mice and $Tlr2^{-/-}$ mice exhibiting less TLR2 expression and 5-HT production, we first investigated whether 5-HT level is increased by activating TLR2 with a synthetic agonist (Pam3CSK4) in GF mice. We administered the agonist i.p. and by oral gavage as per previously reported dosage (45) to examine the changes in EC cell number, *Tph1* expression, and 5-HT levels. We observed an increased EC cell number along with a significant upregulation of *Tph1* expression and 5-HT levels in GF mice by both routes of administration (Fig. 4). However, there was no increase in EC cell number, *Tph1* expression, or colonic 5-HT levels by LPS treatment (Fig. 4). Moreover, we used $Tph1^{-/-}$ mice and administered Pam3CSK4 (i.p.) to confirm whether an increase in 5-HT production by Pam3CSK4 is mediated by *Tph1*. We did not find any significant changes in 5-HT levels in the colon of $Tph1^{-/-}$ mice by Pam3CSK4, compared with Pam3CSK4-treated WT mice, suggesting that Pam3CSK4-mediated activation of TLR2/1 increases 5-HT levels in the gut via *Tph1* upregulation (Supplemental Fig. 2).

Direct activation of TLR2 signaling by Pam3CKS4 in EC cells upregulates Tph1 *and 5-HT levels via NF-κB pathway*

To test the direct effect of TLR signaling in regulating 5-HT production in the gut, we used BON cells, which are a well-established model of human EC cells expressing functional TLR1, 2, and 4 (26). Treatment of BON cells with increasing dosages of Pam3CSK4 (2, 5, and 10 μg/ml) resulted in the upregulation of *Tph1* expression (Fig. 5A) and 5-HT production (Fig. 5B), whereas sodium butyrate (NaB) was used as a positive control in these experiments as per previously described report (22). Conversely, the effect of LPS treatment was NS in inducing changes in *Tph1* expression and 5-HT production (Supplemental Fig. 3). These findings further highlight the vital role of the TLR2/1 signaling pathway in regulating 5-HT production. As TLR signaling cascade activation results in a downstream response, which is mediated by NF-κB and/or AP-1 translocation (24, 46), we sought to assess the signaling pathway to determine the mechanisms behind Tph1 and subsequent 5-HT upregulation. BON-1 cells were pretreated for 1 h with triptolide (NF-κB inhibitor) and SR 11302 (AP-1 inhibitor) (47), followed by treatment with Pam3CSK4. We observed that SR 11302 had no significant effect on Pam3CSK4-stimulated 5-HT production. However, triptolide treatment significantly inhibited 5-HT production in Pam3CSK4-treated cells (Fig. 5C). These findings suggest that TLR2-mediated NF-κB activation is required for 5-HT production. Apart from

FIGURE 4. Activation of TLR2 in GF mice upregulates *Tph1* expression and 5-HT production. GF mice were divided into five groups of four mice each. Mice of group 1 were treated with vehicle (PBS) orally. Mice of group 2 were i.p. treated with 50 μg Pam3CSK4 per injection. Mice of group 3 were treated with 50 μg Pam3CSK4 orally. Mice of group 4 were treated with 1 mg/kg LPS i.p. per injection, and mice of group 5 were treated with 1 mg/kg LPS orally. After 48 h, mice were sacrificed, and the colonic tissues were collected for further analysis. (**A**) Representative micrographs of 5-HT–expressing EC cells following immunostaining (brown) in colonic sections of mice treated with vehicle, Pam3CSK4, and LPS. Arrows indicate 5-HT–positive cells. Colonic sections were visualized using a Nikon Eclipse 80i microscope (original magnification ×10). (**B**) 5-HT–expressing EC cells per 10 crypts in the colon. (**C**) Colonic 5-HT levels (*n* = 3–4 mice per group). (**D**) Colonic *Tph1* expression (fold change). Unpaired Student *t* test was used to analyze statistical differences. Data are represented as either mean or mean ± SEM where applicable. *$p < 0.05$.
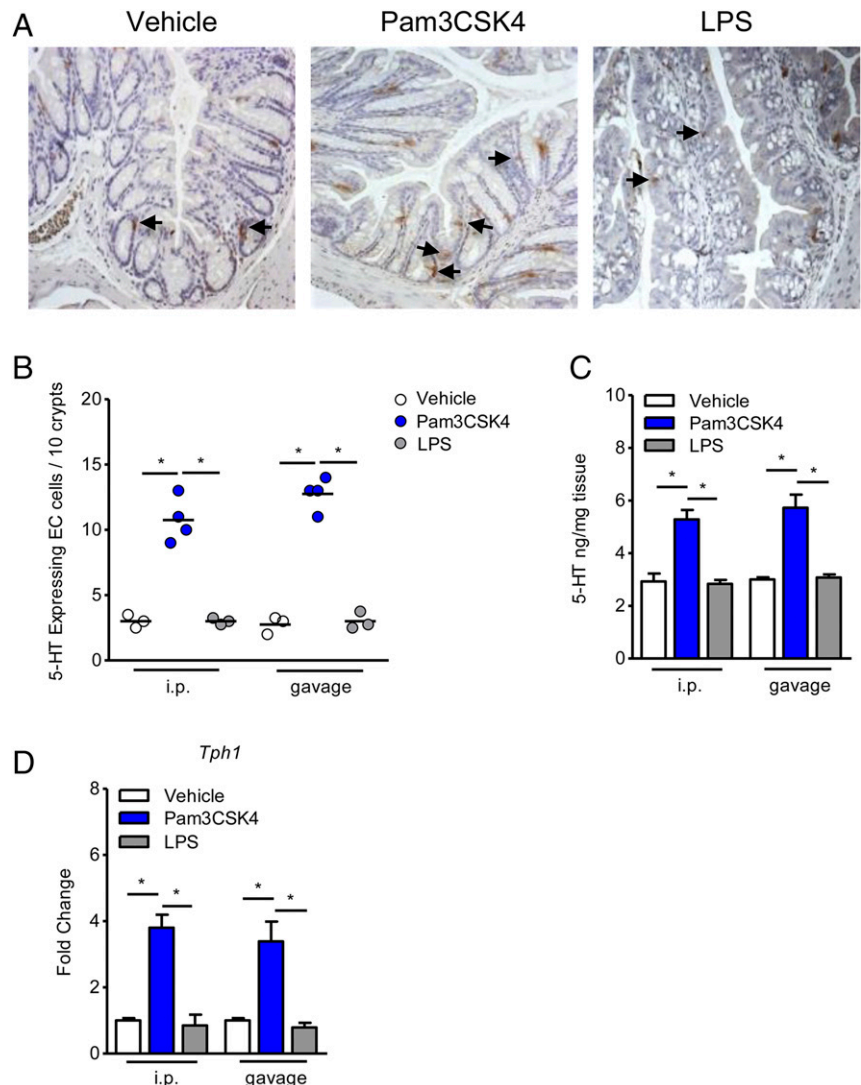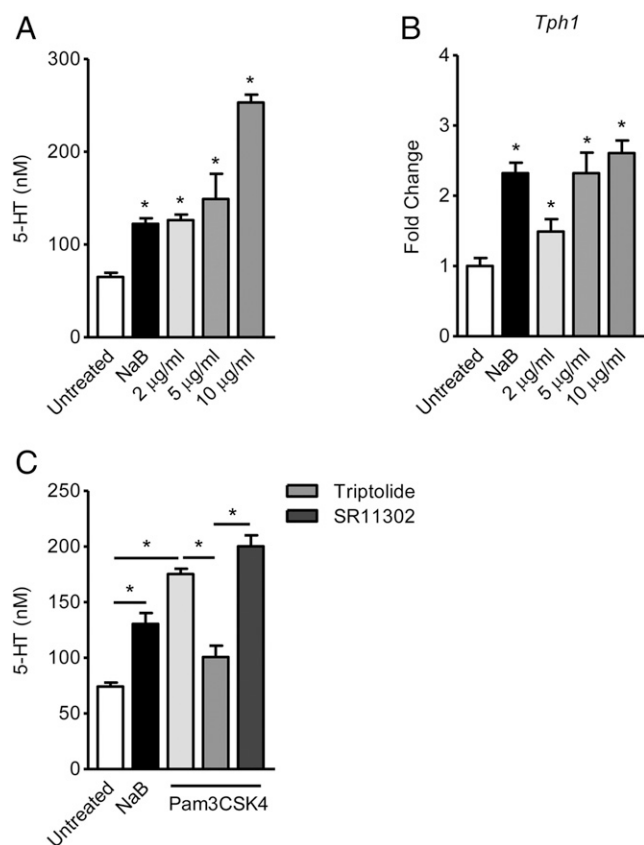
FIGURE 5. Activation of TLR2 by Pam3CSK4 increases 5-HT levels in vitro. BON-1 cells were treated with Pam3CSK4 (2, 5, and 10 μg/ml) for 24 h. The supernatants and cell pellets were collected to access (**A**) 5-HT levels upon Pam3CSK treatment. (**B**) *Tph1* expression normalized to 18s rRNA housekeeping gene determined by quantitative RT-PCR. Sodium butyrate (NaB; 1 mM) was used as a positive control for 5-HT release. (**C**) 5-HT levels after pretreatment with either NF-κB inhibitor (Triptolide: 20 nM) or AP-1 inhibitor (SR-11302: 1 μM) for 1 h and subsequent activation with Pam3CSK4 (10 μg/ml) for 24 h. Where applicable, unpaired Student t test and one-way ANOVA with Dunnett multiple comparisons were used to analyze statistical differences. Data are representative of three independent experiments and represented as mean ± SEM. *$p < 0.05$.

highlighting the central role played by TLR2 in 5-HT signaling and release, these results excluded the possibility of any other contributing TLRs toward 5-HT release.

TLR2 plays an important role in stimulating 5-HT production during T. muris infection

To investigate the role of TLRs in mediating 5-HT release in an enteric infection model, we used the nematode parasite *T. muris* that resides in the large intestine of mice. This parasite is very similar to the human parasite *Trichuris trichiura* and is a commonly used model for studying host immunity in enteric nematode parasite infections. Previously, using *T. muris*–infected mice, we have observed an upregulation of EC cell numbers and 5-HT amount, which was accompanied by the increase in production of colonic Th2 cytokines (11, 12). We first used *Tlr2*$^{-/-}$ mice to elucidate the role of TLR2 in 5-HT production during *T. muris* infection. We observed a significant reduction in EC cell numbers, 5-HT levels, parasite expulsion, and IL-4 levels in *Tlr2*$^{-/-}$ mice infected with *T. muris* at day 16 (Fig. 6A–E), whereas there was no significant difference in IFN-γ and IL-17A production (data not shown). However, naive *Tlr2*$^{-/-}$ mice have lower EC cell numbers and 5-HT levels, and it is difficult to precisely discern the differences between WT and *Tlr2*$^{-/-}$ following the infection.

Thus, we decided to block TLR2 signaling by an additional approach for further determine the role of TLR2 in 5-HT production after *T. muris* infection (Fig. 6F). Previous studies have used anti-TLR2 Ab as a neutralizing agent to block binding of TLR2 ligands (32, 48–50). In our study, anti-TLR2 Ab significantly reduced the number of EC cells and 5-HT production in both naive and infected mice (Fig. 6G–I). Along with increased worm burden in the cecum (Fig. 6J), both IL-4 and IL-13 levels were decreased in the colonic tissues of infected mice with anti-TLR2 Ab treatment (Fig. 6K, 6L). We also observed that anti-TLR2 Ab treatment attenuated IL-13 production, but not IL-4, in noninfected mice. To further elucidate the role of TLR2 in regulating 5-HT production during *T. muris* infection, we sought to explore whether *T. muris* ESPs induce 5-HT production in BON-1 cells. The ESPs exhibited a dose-dependent effect on 5-HT production, where a higher concentration of the ESPs induced more 5-HT production in BON-1 cells (Fig. 7A). In addition, the ESPs showed a direct effect on *Tlr2* mRNA (Fig. 7B) and protein expression (Fig. 7C, 7D), whereas 5-HT levels were attenuated upon TLR2 antagonist treatment (Fig. 7E).

Discussion

Because of the strategic location of EC cells in the mucosal layer, it is very likely that microorganisms in the gut interact with EC cells to stimulate 5-HT in the context of gut health. In this article, we report that TLR2 signaling is necessary to sustain EC cell biology and 5-HT production, whereas disruption of homeostatic equilibrium of microbial community in the gut leads to reduced EC cell number and 5-HT levels.

5-HT has been implicated in the pathophysiology of many GI disorders, including IBD, IBS, and enteric infections (8–13). Changes in EC cell numbers and 5-HT content have been reported in association with two major forms of IBD, Crohn disease and ulcerative colitis (8, 9, 51). In animal models, increased 5-HT levels have been observed in colitis induced by 2,4,6-trinitrobenzenesulfonic acid (TNBS), 2,4-dinitrobenzenesulfonic acid, and DSS (5, 51, 52). *Tph1*$^{-/-}$ mice exhibit reduced severity of colitis while replenishing 5-HT–exacerbated severity of colitis (15). It is also shown that 5-HT plays a key role in the activation of dendritic cells and macrophages to produce proinflammatory cytokines (16, 53, 54). These observations suggest an important role of 5-HT in the pathogenesis of colitis. In IBS, 5-HT release was increased in the patients with diarrhea-predominant IBS, thus rationalizing the use of 5-HT antagonists in treating this subgroup of patients (55). Interestingly, alteration in EC cell number is also observed in many GI infections, including infections with *Salmonella typhimurium*, *Trichinella spiralis*, and *T. muris* (10–13). Thus, it can be surmised that 5-HT is an important enteric signaling molecule, and elucidating the mechanism of 5-HT production is critical in understanding intestinal physiology, pathology, and pathophysiology.

Our present data show that treatment of naive SPF mice with either neomycin or vancomycin significantly reduced 5-HT–expressing EC cell numbers along with 5-HT amount and TLR2 expression in the colon. The major TLR2 ligands characterized thus far are lipoproteins, which are expressed on the outer membrane of Gram-positive bacteria. Our metagenomics analysis revealed that antibiotic treatment decreased mostly the relative abundance of Gram-positive bacteria, which subsequently reduced TLR2 transcripts, EC cell number, and 5-HT levels. It seems likely that these changes resulted from the loss of TLR2 ligands and subsequent loss of byproducts of microbial metabolism (i.e., short-chain fatty acids) because of antibiotic treatment. Along with our data from GF mice study, these findings suggest
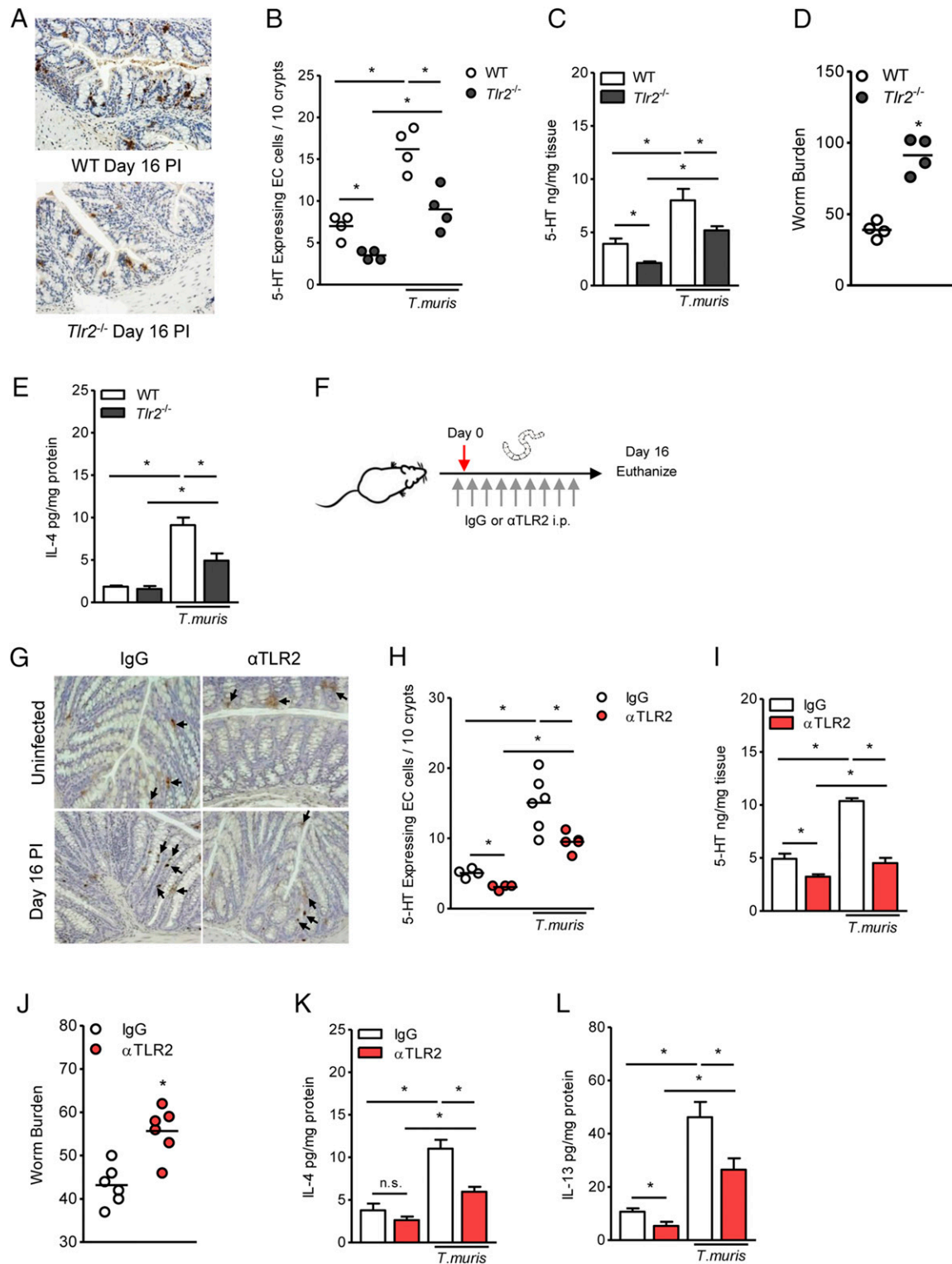
FIGURE 6. $Tlr2^{-/-}$ mice and anti-TLR2 Ab–treated mice exhibit reduction of the colonic 5-HT levels, EC cell number, and attenuated Th2 immune response, along with impairment in host protection during *T. muris* infection. WT and $Tlr2^{-/-}$ mice were infected with ~300 embryonated *T. muris* eggs. (**A**) Representative immunostaining for 5-HT–expressing cells (brown) in the colon of WT and $Tlr2^{-/-}$ mice. Colonic sections were visualized using a Nikon Eclipse 80i microscope (original magnification ×10). (**B**) 5-HT–expressing EC cells in the colon. (**C**) Colonic 5-HT levels. (**D**) Worm burden in the cecum ($n = 4$ per group). (**E**) Colonic IL-4 levels. (**F**) Experimental design: C57BL/6 mice were either treated with 200 μg/kg of IgG or anti-TLR2 Ab (αTLR2) every other day starting from 1 d before infection. In another group, mice were infected with ~300 embryonated *T. muris* eggs while getting treated with either 200 μg/kg of IgG or αTLR2 every other day starting from 1 d before infection. All mice were sacrificed on day 16 postinfection ($n = 4$ per group, anti-IgG and anti-TLR2 Ab without *T. muris*; $n = 6$ per group, anti-IgG and anti-TLR2 Ab with *T. muris*). Red arrow indicates administration of the parasite eggs orally. (**G**) Representative immunostaining for 5-HT–expressing cells (brown) in the colon of anti-IgG–treated mice and anti-TLR2 Ab–treated mice after *T. muris* infection. Arrows indicate 5-HT–positive cells. Colonic sections were visualized using a Nikon Eclipse 80i microscope (original magnification ×10). (**H**) 5-HT–expressing EC cells in the colon. (**I**) Colonic 5-HT levels. (**J**) Worm burden in the cecum. (**K**) Colonic IL-4 levels. (**L**) Colonic IL-13 levels. ($n = 4$–6 mice per group). Unpaired Student *t* test was used to analyze statistical differences. Data are represented as either mean or mean ± SEM where applicable. *$p < 0.05$; n.s., not significant.
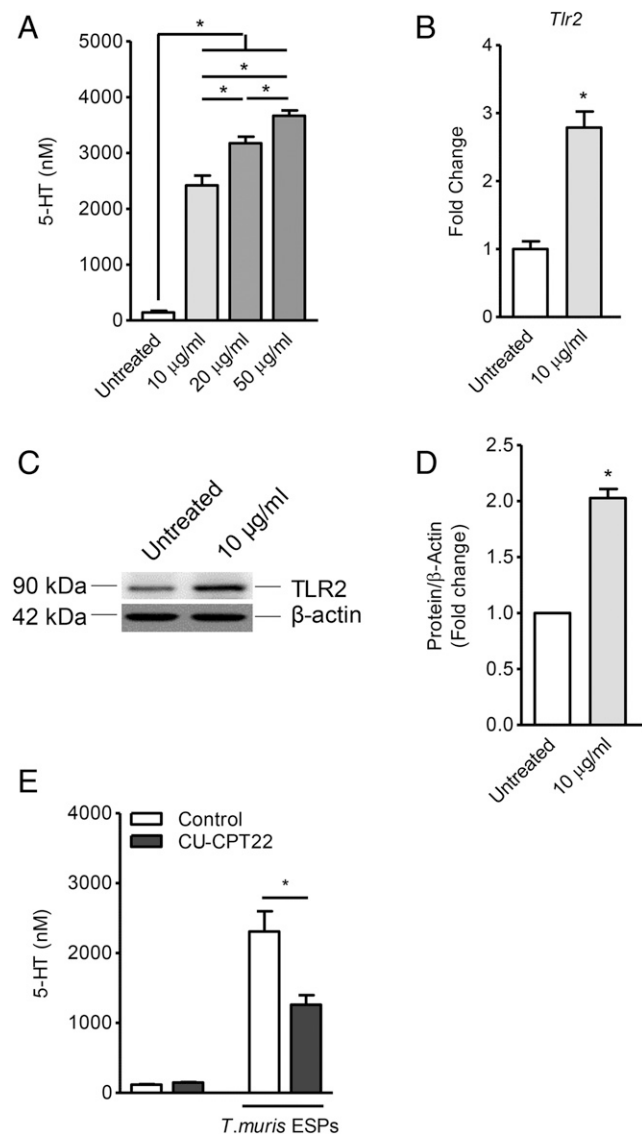
FIGURE 7. *T. muris* ESPs upregulate 5-HT production from human EC cell line (BON-1 cells) by activating TLR2 signaling. BON-1 cells were stimulated with or without *T. muris* ESPs at increasing concentrations (10, 20, and 50 µg/ml) for 24 h to assess 5-HT levels in the culture supernatants and *Tlr2* expression in cells. (**A**) Dose-dependent effect of the ESPs on 5-HT levels in the cell supernatants. (**B**) *Tlr2* mRNA expression upon 24 h of 10 µg/ml of ESPs treatment. (**C**) Representative image of Western blot analysis of TLR2 in BON-1 cell lysates after 24 h of *T. muris* ESP treatment (10 µg/ml). Specific bands for TLR2 were quantified by densitometry. β-actin was used as a loading control. (**D**) Data indicate the relative densities of protein expression from two independent experiments. (**E**) 5-HT levels in the cell supernatants after 1 h of treatment with TLR2 antagonist (CU-CPT22; 1 µM) and subsequent treatment with *T. muris* ESPs (10 µg/ml) for 24 h. Unpaired Student *t* test was used to analyze statistical differences. Data are representative of three independent experiments and represented as mean ± SEM. *$p < 0.05$.

that microbes regulate EC cell biology and 5-HT production via TLR2 signaling pathway, which may subsequently regulate essential 5-HT–related physiological functions.

Apart from recent findings that TLR2 activation decreases 5-HT reuptake by downregulating serotonin reuptake transporter expression and $Tlr2^{-/-}$ mice express an increased level of serotonin reuptake transporter (56), our study revealed that fecal 5-HT levels and *Math1* and *Tph1* expression were decreased in naive $Tlr2^{-/-}$ and $Myd88^{-/-}$ mice. The equivalency between these two mouse

strains suggests that TLR2 deficiency alone is responsible for the observed phenotype. Intestinal epithelial cells are constantly exposed to trillions of microorganisms, and these cells not only recognize and convey important microbial signals through TLRs for a rapid initial response but also work together with microbes to regulate many aspects of GI physiology. Particularly, it is demonstrated that gut microbiota plays a key role in stimulating colonic 5-HT via Tph1 in EC cells, suggesting that microbes require host Tph1 to modulate 5-HT secretion from EC cells (22). Tph1 is responsible for most of 5-HT synthesis in the gut, and our finding shows that TLR2 signaling regulates *Tph1* expression. However, as many leukocytes also respond to microbes through TLR2, and it is noteworthy that mast cells and T cells express Tph1 (57), we have created chimeric mice to demonstrate the observed phenotypes in $Tlr2^{-/-}$ mice. In our study, the importance of TLR2 signaling within the nonhematopoietic cells, most likely intestinal epithelial cells, on 5-HT production appears reasonable to postulate that the epithelial cells have evolved to sense and respond to essential microbial stimuli via TLR2 to promote 5-HT secretion for rapid initial responses. It can also be mentioned that we are unable to exclude the role of radioresistant hematopoietic cells, and further studies with cell-specific deletions are warranted to elucidate the exact cell type in the nonhematopoietic compartment.

Our present data from *T. muris* infection model provide evidence that TLR2 stands out as a key player in regulating EC cell biology during infection. First, we observed significantly lower numbers of EC cells and 5-HT levels in $Tlr2^{-/-}$ mice during *T. muris* infection as compared with the WT mice, and these findings were supported by the studies with anti-TLR2 Ab treatment. Aside from the neutralizing effects of anti-TLR2 Ab in vitro (58), previous studies have also demonstrated the neutralizing efficacy in vivo (25, 49, 50, 59). It is worth mentioning here that i.p. injection of the Ab significantly downregulated mucosal TLR2 expression along with attenuating inflammation in the DSS-colitis model (59), further supporting the view that anti-TLR2 Ab treatment via the i.p. route may have therapeutic potential to efficiently target TLR2 during infectious and inflammatory diseases. Thus, taken together, these findings suggest an important role for TLR2 in 5-HT production during *T. muris* infection.

Previously, it has been shown that *T. muris* induces a strong Th2 response and expels the worms by day 21 postinfection in resistant strain of mice (C57BL/6 and BALB/c) (12, 43). Using *T. muris* model, we have previously observed higher 5-HT levels and EC cell numbers in C57BL/6 mice, which are resistant to infection by expelling worms through a Th2-type immune response, as compared with susceptible AKR mice that developed chronic infection with the generation of a Th1 response (11). In the current study, we demonstrated that TLR2 activation generates a Th2-type immune response and mediates microbial signals to stimulate 5-HT, which can subsequently act on enteric neurons via 5-HT receptors for worm expulsion while neutralizing TLR2 signaling by anti-TLR2 Ab reversed the observed phenotype. In addition, IL-13 levels were decreased in noninfected mice treated with anti-TLR2 Ab. We have previously shown that IL-13 plays an important role in EC cell biology. Recombinant mouse IL-13 (rmIL-13) increased EC cell number and 5-HT amount in naive $Il13^{-/-}$ mice, whereas BON-1 cells produced more 5-HT via IL-13Rα1 upon recombinant human IL-13 (rhIL-13) treatment (38). The knowledge of the mechanisms by which IL-13 regulates TLR2 signaling or vice versa in 5-HT production is still modest.

Several studies demonstrated modulation of TLR expression and signaling by bioactive molecules released by helminths. ESPs of *Hymenolepis diminuta* increase TLR2 and TLR4 expression in the intestine (60). Another study has demonstrated that *Schistosoma*

japonicum Ags induce high expression of TLR2 on murine dendritic cells (61). The ESPs of *T. muris* are shown to be very immunogenic (43), and in our present study, we observed *T. muris* ESPs directly upregulate 5-HT production via TLR2 from BON-1 cell in an NF-κB–dependent manner. In addition to influencing EC cells and subsequent 5-HT production through ESPs, *T. muris* may also indirectly influence 5-HT production via altering the microbial composition. Recently, it is demonstrated that chronic infection of *T. muris* causes a significant impact on gut microbial composition (20), suggesting an important role of TLR2 signaling in the regulation of 5-HT production and Th2 responses in the context of host defense in *T. muris* infection. The role of TLR2 in the host defense is also investigated in other enteric infections including infection with bacterial pathogens. It has been shown that $Tlr2^{-/-}$ mice infected with *Citrobacter rodentium* suffered a lethal colitis along with impaired epithelial function but not increased pathogen burden (62). Another study demonstrated a lower degree of gastric *Helicobacter pylori* colonization and more severe gastric immunopathology in $Tlr2^{-/-}$ mice (63). In this study, we found that ESP components increased the expression of TLR2 and 5-HT levels. However, further studies are required to elucidate how ESP components upregulates TLR2 expression, which corresponds to the increase in 5-HT level.

Altogether, this study identifies a novel and important role of TLR2 in gut function. In addition to enhancing our understanding of the EC cell biology, this study provides important information on the role of TLR2-mediated signaling in the interaction of EC cells with resident microbiota and an invasive pathogen in the context of gut physiology and pathophysiology. TLR2 may serve as a novel target for modulating 5-HT synthesis and release in various health disorders that display aberrant 5-HT signaling.

Acknowledgments

Disclosures

The authors have no financial conflicts of interest.

References

1. Sharkey, K. A., and G. M. Mawe. 2002. Neuroimmune and epithelial interactions in intestinal inflammation. *Curr. Opin. Pharmacol.* 2: 669–677.
2. Rindi, G., and G. Klöppel. 2004. Endocrine tumors of the gut and pancreas tumor biology and classification. *Neuroendocrinology* 80(Suppl. 1): 12–15.
3. Kim, D. Y., and M. Camilleri. 2000. Serotonin: a mediator of the brain-gut connection. *Am. J. Gastroenterol.* 95: 2698–2709.
4. Bertrand, P. P., and R. L. Bertrand. 2010. Serotonin release and uptake in the gastrointestinal tract. *Auton. Neurosci.* 153: 47–57.
5. Manocha, M., and W. I. Khan. 2012. Serotonin and GI disorders: an update on clinical and experimental studies. *Clin. Transl. Gastroenterol.* 3: e13.
6. Banskota, S., S. C. Regmi, J. Gautam, P. Gurung, Y. J. Lee, S. K. Ku, J. H. Lee, J. Lee, H. W. Chang, S. J. Park, and J. A. Kim. 2017. Serotonin disturbs colon epithelial tolerance of commensal *E. coli* by increasing NOX2-derived superoxide. *Free Radic. Biol. Med.* 106: 196–207.
7. Mawe, G. M., and J. M. Hoffman. 2013. Serotonin signalling in the gut--functions, dysfunctions and therapeutic targets. [Published erratum appears in 2013 *Nat. Rev. Gastroenterol. Hepatol.* 10: 564.] *Nat. Rev. Gastroenterol. Hepatol.* 10: 473–486.
8. Belai, A., P. B. Boulos, T. Robson, and G. Burnstock. 1997. Neurochemical coding in the small intestine of patients with Crohn's disease. *Gut* 40: 767–774.
9. Coates, M. D., C. R. Mahoney, D. R. Linden, J. E. Sampson, J. Chen, H. Blaszyk, M. D. Crowell, K. A. Sharkey, M. D. Gershon, G. M. Mawe, and P. L. Moses. 2004. Molecular defects in mucosal serotonin content and decreased serotonin reuptake transporter in ulcerative colitis and irritable bowel syndrome. *Gastroenterology* 126: 1657–1664.
10. Grøndahl, M. L., G. M. Jensen, C. G. Nielsen, E. Skadhauge, J. E. Olsen, and M. B. Hansen. 1998. Secretory pathways in *Salmonella* Typhimurium-induced fluid accumulation in the porcine small intestine. *J. Med. Microbiol.* 47: 151–157.
11. Motomura, Y., J. E. Ghia, H. Wang, H. Akiho, R. T. El-Sharkawy, M. Collins, Y. Wan, J. T. McLaughlin, and W. I. Khan. 2008. Enterochromaffin cell and 5-hydroxytryptamine responses to the same infectious agent differ in Th1 and Th2 dominant environments. *Gut* 57: 475–481.
12. Wang, H., J. Steeds, Y. Motomura, Y. Deng, M. Verma-Gandhu, R. T. El-Sharkawy, J. T. McLaughlin, R. K. Grencis, and W. I. Khan. 2007. CD4+ T cell-mediated immunological control of enterochromaffin cell hyperplasia and 5-hydroxytryptamine production in enteric infection. *Gut* 56: 949–957.
13. Wheatcroft, J., D. Wakelin, A. Smith, C. R. Mahoney, G. Mawe, and R. Spiller. 2005. Enterochromaffin cell hyperplasia and decreased serotonin transporter in a mouse model of postinfectious bowel dysfunction. *Neurogastroenterol. Motil.* 17: 863–870.
14. Shajib, M. S., U. Chauhan, S. Adeeb, Y. Chetty, D. Armstrong, S. L. Halder, J. K. Marshall, and W. I. Khan. 2018. Characterization of serotonin signaling components in patients with inflammatory bowel disease. *J. Can. Assoc. Gastroenterol.* Available at: https://doi.org/10.1093/jcag/gwy039.
15. Ghia, J. E., N. Li, H. Wang, M. Collins, Y. Deng, R. T. El-Sharkawy, F. Côté, J. Mallet, and W. I. Khan. 2009. Serotonin has a key role in pathogenesis of experimental colitis. *Gastroenterology* 137: 1649–1660.
16. Kim, J. J., H. Wang, J. D. Terc, B. Zambrowicz, Q. M. Yang, and W. I. Khan. 2015. Blocking peripheral serotonin synthesis by telotristat etiprate (LX1032/LX1606) reduces severity of both chemical- and infection-induced intestinal inflammation. *Am. J. Physiol. Gastrointest. Liver Physiol.* 309: G455–G465.
17. Liévin-Le Moal, V., and A. L. Servin. 2006. The front line of enteric host defense against unwelcome intrusion of harmful microorganisms: mucins, antimicrobial peptides, and microbiota. *Clin. Microbiol. Rev.* 19: 315–337.
18. Bancroft, A. J., K. S. Hayes, and R. K. Grencis. 2012. Life on the edge: the balance between macrofauna, microflora and host immunity. *Trends Parasitol.* 28: 93–98.
19. Hayes, K. S., A. J. Bancroft, M. Goldrick, C. Portsmouth, I. S. Roberts, and R. K. Grencis. 2010. Exploitation of the intestinal microflora by the parasitic nematode Trichuris muris. *Science* 328: 1391–1394.
20. Houlden, A., K. S. Hayes, A. J. Bancroft, J. J. Worthington, P. Wang, R. K. Grencis, and I. S. Roberts. 2015. Chronic Trichuris muris infection in C57BL/6 mice causes significant changes in host microbiota and metabolome: effects reversed by pathogen clearance. *PLoS One* 10: e0125945.
21. Klementowicz, J. E., M. A. Travis, and R. K. Grencis. 2012. Trichuris muris: a model of gastrointestinal parasite infection. *Semin. Immunopathol.* 34: 815–828.
22. Yano, J. M., K. Yu, G. P. Donaldson, G. G. Shastri, P. Ann, L. Ma, C. R. Nagler, R. F. Ismagilov, S. K. Mazmanian, and E. Y. Hsiao. 2015. Indigenous bacteria from the gut microbiota regulate host serotonin biosynthesis. [Published erratum appears in 2015 Cell 163: 258.] *Cell* 161: 264–276.
23. Fukumoto, S., M. Tatewaki, T. Yamada, M. Fujimiya, C. Mantyh, M. Voss, S. Eubanks, M. Harris, T. N. Pappas, and T. Takahashi. 2003. Short-chain fatty acids stimulate colonic transit via intraluminal 5-HT release in rats. *Am. J. Physiol. Regul. Integr. Comp. Physiol.* 284: R1269–R1276.
24. Akira, S., and K. Takeda. 2004. Toll-like receptor signalling. *Nat. Rev. Immunol.* 4: 499–511.
25. Price, A. E., K. Shamardani, K. A. Lugo, J. Deguine, A. W. Roberts, B. L. Lee, and G. M. Barton. 2018. A map of toll-like receptor expression in the intestinal epithelium reveals distinct spatial, cell type-specific, and temporal patterns. *Immunity* 49: 560–575.e6.
26. Bogunovic, M., S. H. Davé, J. S. Tilstra, D. T. Chang, N. Harpaz, H. Xiong, L. F. Mayer, and S. E. Plevy. 2007. Enteroendocrine cells express functional toll-like receptors. *Am. J. Physiol. Gastrointest. Liver Physiol.* 292: G1770–G1783.
27. Syed, S. A., F. J. Whelan, B. Waddell, H. R. Rabin, M. D. Parkins, and M. G. Surette. 2016. Reemergence of lower-airway microbiota in lung transplant patients with cystic fibrosis. *Ann. Am. Thorac. Soc.* 13: 2132–2142.
28. Bartram, A. K., M. D. Lynch, J. C. Stearns, G. Moreno-Hagelsieb, and J. D. Neufeld. 2011. Generation of multimillion-sequence 16S rRNA gene libraries from complex microbial communities by assembling paired-end illumina reads. [Published erratum appears in 2011 *Appl. Environ. Microbiol.* 77: 5569.] *Appl. Environ. Microbiol.* 77: 3846–3852.
29. Whelan, F. J., and M. G. Surette. 2017. A comprehensive evaluation of the sl1p pipeline for 16S rRNA gene sequencing analysis. *Microbiome* 5: 100.
30. Ye, Y. 2011. Identification and quantification of abundant species from pyrosequences of 16S rRNA by consensus alignment. *Proceedings (IEEE Int. Conf. Bioinformatics Biomed).* 2010: 153–157.
31. Reigstad, C. S., C. E. Salmonson, J. F. Rainey, III, J. H. Szurszewski, D. R. Linden, J. L. Sonnenburg, G. Farrugia, and P. C. Kashyap. 2015. Gut microbes promote colonic serotonin production through an effect of short-chain fatty acids on enterochromaffin cells. *FASEB J.* 29: 1395–1403.
32. Yan, J., F. Hua, H. Z. Liu, H. Z. Yang, and Z. W. Hu. 2012. Simultaneous TLR2 inhibition and TLR9 activation synergistically suppress tumor metastasis in mice. *Acta Pharmacol. Sin.* 33: 503–512.
33. Ortíz-Alvarado, R., O. Guzmán-Quevedo, R. Mercado-Camargo, T. Haertle, C. Vignes, and F. Bolaños-Jiménez. 2006. Expression of tryptophan hydroxylase in developing mouse taste papillae. *FEBS Lett.* 580: 5371–5376.
34. Rahman, A., P. Sobia, N. Gupta, L. V. Kaer, and G. Das. 2014. *Mycobacterium tuberculosis* subverts the TLR-2-MyD88 pathway to facilitate its translocation into the cytosol. *PLoS One* 9: e86886.
35. Wang, F., J. Wang, D. Liu, and Y. Su. 2010. Normalizing genes for real-time polymerase chain reaction in epithelial and nonepithelial cells of mouse small intestine. *Anal. Biochem.* 399: 211–217.
36. Drobits, B., M. Holcmann, N. Amberg, M. Swiecki, R. Grundtner, M. Hammer, M. Colonna, and M. Sibilia. 2012. Imiquimod clears tumors in mice independent of adaptive immunity by converting pDCs into tumor-killing effector cells. *J. Clin. Invest.* 122: 575–585.
37. Xue, Y., H. Zhang, X. Sun, and M. J. Zhu. 2016. Metformin improves ileal epithelial barrier function in interleukin-10 deficient mice. *PLoS One* 11: e0168670.

38. Manocha, M., M. S. Shajib, M. M. Rahman, H. Wang, P. Rengasamy, M. Bogunovic, M. Jordana, L. Mayer, and W. I. Khan. 2013. IL-13-mediated immunological control of enterochromaffin cell hyperplasia and serotonin production in the gut. *Mucosal Immunol.* 6: 146–155.

39. Johnson, C. M., and R. I. Tapping. 2007. Microbial products stimulate human toll-like receptor 2 expression through histone modification surrounding a proximal NF-kappaB-binding site. *J. Biol. Chem.* 282: 31197–31205.

40. Stephens, A. S., S. R. Stephens, and N. A. Morrison. 2011. Internal control genes for quantitative RT-PCR expression analysis in mouse osteoblasts, osteoclasts and macrophages. *BMC Res. Notes* 4: 410.

41. Wang, H., J. J. Kim, E. Denou, A. Gallagher, D. J. Thornton, M. S. Shajib, L. Xia, J. D. Schertzer, R. K. Grencis, D. J. Philpott, and W. I. Khan. 2015. New role of Nod proteins in regulation of intestinal goblet cell response in the context of innate host defense in an enteric parasite infection. *Infect. Immun.* 84: 275–285.

42. Bradford, M. M. 1976. A rapid and sensitive method for the quantitation of microgram quantities of protein utilizing the principle of protein-dye binding. *Anal. Biochem.* 72: 248–254.

43. Else, K., and D. Wakelin. 1989. Genetic variation in the humoral immune responses of mice to the nematode Trichuris muris. *Parasite Immunol.* 11: 77–90.

44. Herman, A. C., D. A. Monlish, M. P. Romine, S. T. Bhatt, S. Zippel, and L. G. Schuettpelz. 2016. Systemic TLR2 agonist exposure regulates hematopoietic stem cells via cell-autonomous and cell-non-autonomous mechanisms. *Blood Cancer J.* 6: e437.

45. Sanchez, P. J., J. A. McWilliams, C. Haluszczak, H. Yagita, and R. M. Kedl. 2007. Combined TLR/CD40 stimulation mediates potent cellular immunity by regulating dendritic cell expression of CD70 in vivo. *J. Immunol.* 178: 1564–1572.

46. O'Neill, L. A., D. Golenbock, and A. G. Bowie. 2013. The history of toll-like receptors - redefining innate immunity. *Nat. Rev. Immunol.* 13: 453–460.

47. Yinjun, L., J. Jie, and W. Yungui. 2005. Triptolide inhibits transcription factor NF-kappaB and induces apoptosis of multiple myeloma cells. *Leuk. Res.* 29: 99–105.

48. Meng, G., M. Rutz, M. Schiemann, J. Metzger, A. Grabiec, R. Schwandner, P. B. Luppa, F. Ebel, D. H. Busch, S. Bauer, et al. 2004. Antagonistic antibody prevents toll-like receptor 2-driven lethal shock-like syndromes. *J. Clin. Invest.* 113: 1473–1481.

49. Arslan, F., M. B. Smeets, L. A. O'Neill, B. Keogh, P. McGuirk, L. Timmers, C. Tersteeg, I. E. Hoefer, P. A. Doevendans, G. Pasterkamp, and D. P. de Kleijn. 2010. Myocardial ischemia/reperfusion injury is mediated by leukocytic toll-like receptor-2 and reduced by systemic administration of a novel anti-toll-like receptor-2 antibody. *Circulation* 121: 80–90.

50. Yang, H.-Z., B. Cui, H.-Z. Liu, Z.-R. Chen, H.-M. Yan, F. Hua, and Z.-W. Hu. 2009. Targeting TLR2 attenuates pulmonary inflammation and fibrosis by reversion of suppressive immune microenvironment. *J. Immunol.* 182: 692–702.

51. Ahonen, A., K. Kyösola, and O. Penttilä. 1976. Enterochromaffin cells in macrophages in ulcerative colitis and irritable colon. *Ann. Clin. Res.* 8: 1–7.

52. Khan, W. I., Y. Motomura, H. Wang, R. T. El-Sharkawy, E. F. Verdu, M. Verma-Gandhu, B. J. Rollins, and S. M. Collins. 2006. Critical role of MCP-1 in the pathogenesis of experimental colitis in the context of immune and enterochromaffin cells. *Am. J. Physiol. Gastrointest. Liver Physiol.* 291: G803–G811.

53. Kwon, Y. H., H. Wang, E. Denou, J. E. Ghia, L. Rossi, M. E. Fontes, S. P. Bernier, M. S. Shajib, S. Banskota, S. M. Collins, et al. 2019. Modulation of gut microbiota composition by serotonin signaling influences intestinal immune response and susceptibility to colitis. *Cell. Mol. Gastroenterol. Hepatol.* DOI: 10.1016/j.jcmgh.2019.01.004.

54. Li, N., J. E. Ghia, H. Wang, J. McClemens, F. Cote, Y. Suehiro, J. Mallet, and W. I. Khan. 2011. Serotonin activates dendritic cell function in the context of gut inflammation. *Am. J. Pathol.* 178: 662–671.

55. Bearcroft, C. P., D. Perrett, and M. J. Farthing. 1998. Postprandial plasma 5-hydroxytryptamine in diarrhoea predominant irritable bowel syndrome: a pilot study. *Gut* 42: 42–46.

56. Latorre, E., E. Layunta, L. Grasa, M. Castro, J. Pardo, F. Gomollón, A. I. Alcalde, and J. E. Mesonero. 2016. Intestinal serotonin transporter inhibition by toll-like receptor 2 activation. A feedback modulation. *PLoS One* 11: e0169303.

57. Nowak, E. C., V. C. de Vries, A. Wasiuk, C. Ahonen, K. A. Bennett, I. Le Mercier, D.-G. Ha, and R. J. Noelle. 2012. Tryptophan hydroxylase-1 regulates immune tolerance and inflammation. *J. Exp. Med.* 209: 2127–2135.

58. Pathak, S. K., S. Basu, K. K. Basu, A. Banerjee, S. Pathak, A. Bhattacharyya, T. Kaisho, M. Kundu, and J. Basu. 2007. Direct extracellular interaction between the early secreted antigen ESAT-6 of *Mycobacterium tuberculosis* and TLR2 inhibits TLR signaling in macrophages. *Nat. Immunol.* 8: 610–618.

59. Dong, L., J. Li, Y. Liu, W. Yue, and X. Luo. 2012. Toll-like receptor 2 monoclonal antibody or/and Toll-like receptor 4 monoclonal antibody increase counts of Lactobacilli and Bifidobacteria in dextran sulfate sodium-induced colitis in mice. *J. Gastroenterol. Hepatol.* 27: 110–119.

60. Kane, C. M., L. Cervi, J. Sun, A. S. McKee, K. S. Masek, S. Shapira, C. A. Hunter, and E. J. Pearce. 2004. Helminth antigens modulate TLR-initiated dendritic cell activation. *J. Immunol.* 173: 7454–7461.

61. Gao, Y., M. Zhang, L. Chen, M. Hou, M. Ji, and G. Wu. 2012. Deficiency in TLR2 but not in TLR4 impairs dendritic cells derived IL-10 responses to schistosome antigens. *Cell. Immunol.* 272: 242–250.

62. Gibson, D. L., C. Ma, C. M. Rosenberger, K. S. Bergstrom, Y. Valdez, J. T. Huang, M. A. Khan, and B. A. Vallance. 2008. Toll-like receptor 2 plays a critical role in maintaining mucosal integrity during *Citrobacter* rodentium-induced colitis. *Cell. Microbiol.* 10: 388–403.

63. Sun, X., M. Zhang, M. El-Zataari, S. Y. Owyang, K. A. Eaton, M. Liu, Y. M. Chang, W. Zou, and J. Y. Kao. 2013. TLR2 mediates *Helicobacter pylori*-induced tolerogenic immune response in mice. *PLoS One* 8: e74595.